Extracellular Vesicle 6 (2025) 100084

Contents lists available at ScienceDirect

Extracellular Vesicle

journal homepage: www.elsevier.com/locate/vesic

Using common features of viruses and EVs for a novel EV-based lateral flow test for HIV

Casey Scott-Weathers [a], Kaitlyn King [a], Gary Baisa [a], John Hural [b], Kimberly Luke [a,*]

[a] Intuitive Biosciences, Inc. Madison, WI, USA
[b] Vaccine and Infectious Disease Division, Fred Hutchinson Cancer Center, Seattle, USA

A B S T R A C T

The similarities between extracellular vesicles (EVs) and viruses make them challenging to distinguish and separate into unique populations. A novel lateral flow test has been developed by utilizing these shared properties to improve at-home testing for HIV. By targeting EVs released from HIV infected cells (HIV-EVs) and HIV virus particles for immunocapture, which share common transmembrane proteins like tetraspanins, HIV proteins can be concentrated from blood samples in a lateral flow device. Others have described immunocapture of EVs by lateral flow; here we describe capture and lysis for downstream detection of specific HIV cargo for a sensitive antigen-only HIV test. We found that HIV antigens p24 and Nef are detected early in infection and may significantly improve the sensitivity of an at-home test format by utilizing EVs as a novel reservoir of HIV antigens.

1. Introduction

The similarities between extracellular vesicles (EVs) and viruses make them challenging to distinguish and separate into unique populations. As reviewed by Nolte-'t Hoen et al. in 2016, retroviruses and EVs can be "almost impossible to distinguish" and EVs generated by virally infected cells may contain viral proteins and nucleic acid cargo that can fall under the definition of a noninfectious viral particle.[1] While this overlap between EVs and retroviruses may be frustrating when attempting to parse the basic biology of retrovirus infection and the antiviral response, it is also a similarity that can be exploited for detection of infection. It has been shown that during the production and assembly of human immunodeficiency virus (HIV), tetraspanins are incorporated into the viral membrane,[2–4] and this assembly takes place at endosome like domains, where EVs are released from the cell.[5] Similarly, HIV proteins including p24, Nef, and Tat can be incorporated into either HIV virions or EVs released from HIV-infected cells (HIV-EVs).[6–9]

EVs produced by HIV-infected cells (HIV-EVs) are present at high levels in the plasma of people living with HIV.[10] Most HIV-positive patients, including those on anti-retroviral therapy (ART) who have undetectable RNA levels, express HIV proteins from viral reservoirs and defective proviruses. Consequently, low levels of viral proteins can be detected in plasma even when the infection is considered repressed (i.e., <20 viral copies/mL).[9–12] Likewise, HIV viral proteins are present in EVs isolated from the blood[13–16] and urine[17] of both viremic and non-viremic HIV + patients. The presence and persistence of HIV proteins in EVs provides a potential means for diagnosis of acute and chronic HIV infection.

The similarities between EVs from HIV-infected cells and viral particles can be utilized to improve the test options available for at-home testing. The hypothesis is that concentration of HIV biomarkers may be increased by selection of tetraspanin containing vesicles first. These may include EVs from the host cell, from HIV- infected cells, or HIV virus particles themselves, whether they are infectious or defective. Biomarkers or antigens contained within EVs are not subjected to interference from host antibodies, which is a technical problem for at-home test methods. Currently there is only one FDA-approved diagnostic for self-testing, the OraQuick® in-home HIV test, with 91.7 % sensitivity.[18] This test detects the presence of antibodies to HIV-1/2 but is only recommended for use 3 months after a risk event. Laboratory based testing, including 4th generation antigen/antibody tests and nucleic acid tests (NATs), can detect infection even earlier (i.e., 10–33 days), but are not available for at-home testing.[19]

The HIV antigens present in HIV-EVs are an appealing target for an improved at-home test for HIV, but detection of low abundance proteins typically requires conditions that cannot be achieved in at-home tests. However, as demonstrated in this research, two additional reservoirs of HIV antigens can be accessed by utilizing key features of EVs: 1) HIV-EVs and HIV virions contain tetraspanins that can be immunocaptured to enrich EV and HIV particles in a lateral-flow assay and 2) abundance of HIV antigens in HIV-EVs are higher than that of the same antigens freely

* Corresponding author. Intuitive Biosciences, Madison, WI, USA.
E-mail address: kluke@intuitivebio.com (K. Luke).

https://doi.org/10.1016/j.vesic.2025.100084
Received 17 December 2024; Received in revised form 3 June 2025; Accepted 11 June 2025
Available online 13 June 2025

circulating in whole blood, which allows for earlier and more robust detection.[20] By possibly detecting the virion and HIV-EV antigens in addition to those already circulating in the blood, a more sensitive antigen-only test compatible with an at-home lateral flow format is possible. We propose not to try to distinguish between the virus and the EV, but to detect them both for a more sensitive HIV test that can be used earlier after a risk event.

2. Materials and methods

Cell Culture. H9 (ATCC catalog no. HTB-176) and U937[21] (ATCC CRL-1593.2) cells were cultured in RPMI 1640 supplemented with 10 % FBS, 10 mM HEPES and 10 μg/mL Gentamicin solution. H9MN FI cells were a kind gift from Dr. H. Imamichi (NIAID, Clinical and Molecular Retrovirology Section). U1 cells were obtained through the NIH HIV Reagent Program, Division of AIDS, NIAID, NIH: Human Immunodeficiency Virus Type 1 (HIV-1) Infected U937 Cells (U1), ARP-165, contributed by Dr. Thomas Folks. All cell lines underwent bi-annual mycoplasma testing and annual STR fingerprinting(Cell Line Genetics, Madison, WI). Cells were incubated in FBS-free RPMI 1640 in T-75 flasks until cellular confluence reached roughly 80 %, approximately 48 h.

Plasma. Plasma samples were remnants from the HVTN505 clinical trial shared under a collaboration with Dr. John Hural with the HIV Vaccine Trial Network under NCT00865566. Ten HIV- samples from Visit 7, Day 546 of the trial, 4 weeks after the 4th administration of placebo. These samples were selected to have the greatest chance of vaccine induced seropositivity or antibody interference. The 20 HIV + samples were collected from volunteers 8 weeks after their diagnosis, which will vary for each volunteer on the overall trial schedule. Volunteers were offered antiretroviral therapy; additional information according to each sample can be found in Supplemental Tables 1 and 2

Additional "Normal" human plasma used as controls for Western blots or ELISA were acquired from Precision for Medicine (Frederick, MD) as a confirmed HIV negative sample. A seroconversion panel (0600-0271/Batch 10571150) was acquired from SeraCare (Milford, MA). This panel was collected from a single person over 25 days in 2015 during the development of an HIV infection with reported values from FDA-approved HIV diagnostic tests. No samples were from individuals treated with ART.

EV enrichment by size exclusion chromatography and resin separation. For cell culture EV enrichment, size exclusion chromatography (SEC) was used followed by concentration. Briefly, 100 mL of cell culture media was centrifuged at 300×*g* for 10 min to pellet cells followed by a concentration of the resulting supernatant by 100 kDa molecular weight cut-off (MWCO) filter columns Sartorius Vivaspin 100 (Marlborough, MA). The resulting retentate was added to an Izon qEV Gen 2 35 nm SEC columns and collected using an automated fraction collector. For enrichment of EVs from human plasma, a resin-based method (Cat. No. 60400) was used from Norgen Biotek (Ontario, Canada). A total of 250 μL of each plasma sample was enriched following the manufacturer's instructions resulting in approximately 200 μL of enriched EVs.

EV Characterization. Characterization of EVs was performed in line with the Minimal information for studies of extracellular vesicles (MISEV2023) recommendations including nanoparticle tracking analysis (NTA) using a NanoSight NS300 from Malvern Panalytical (Westborough, MA) or tunable resistive pulse sensing (TRPS) using an Izon Exoid (Medford, MA) for size and particle concentration. Protein concentration was determined by micro-BCA following the manufacturer's instructions (Product Number 23235), Thermo Scientific (Waltham, MA).

Tunable Resistive Pulse Sensing. Isolated extracellular vesicles were characterized using an Izon Exoid (Izon, Cambridge, MA, USA) by measuring the concentration (particles/mL), size-distribution, and particle diameter. The tunable resistive pulse sensing (TRPS) technology detects individual particles by driving particles through a pore using a combination of electrophoretic and convective flow induced by applied voltage and external pressure across the pore. Voltage, stretch, pressure, and baseline current were calibrated. The data analysis was performed with IZON software.

Western Analysis. Automated Western analysis was performed using the Simple Western Abby and a 12–230 kDa Separation Module (Bio Techne) to resolve EV proteins by size. Antibodies for p24 (sc-69727, Santa Cruz), Nef (R0026, custom rabbit monoclonal), and TSG101 (NBP2-67884, Novus Biologicals) were detected using either anti-rabbit or anti-mouse detection modules (Bio Techne) for a semi-quantitative comparison. Area under the curve (AUC) for each protein band was determined using the Compass software (ver. 6.1.0) included in the Abby system. Expected molecular weight for each protein biomarker was compared to that of a recombinant protein control or overexpression lysate.

Transmission Electron Microscopy. 5 μl of enriched extracellular vesicle suspension in PBS was added onto bare metal electron microscopy for 1 min. The grid was blotted dry with filter paper and 10 μL of distilled water was added for 1 min. The water droplet was removed by filter paper and 5 μL of Nano-W™ Methylamine Tungstate (Nanoprobes, Inc. Yaphank, NY) was added, the grid was air dried for 5 min. Grids were then visualized using a transmission electron microscope (FEI CM120, FEI Company Hillsboro, OR).

Fluorescent conjugation. Anti-p24 antibody (sc-69727, Santa Cruz) and anti-Nef antibody (R0026, custom rabbit monoclonal) were conjugated to Alexa-Fluor 647 NHS ester (A37573, Life Technologies) per the manufacturer's instructions. Conjugation was confirmed using a Genesys 30 spectrophotometer (Thermo Scientific, Waltham, MA).

Stochastic optical reconstruction microscopy. EVs were captured, permeabilized as necessary, immunolabelled, and imaged using the EV Profiler 2 Kit (Application Kit™: EV Profiler 2, ONI) by using the direct stochastic optical reconstruction microscopy (dSTORM) technique following the manufacturer's instructions. The following antibodies were used, either provided in the kit or from in-house conjugation as noted in the fluorescent conjugation section above; anti-CD81 (kit, 647 emission), anti-CD63 (kit, 561 emission) and anti-CD9 (kit, 488 emission), Anti-tetraspanin Trio (kit, 561 emission). Freshly prepared dSTORM-imaging buffer was added prior to image acquisition. Images were captured on the Nanoimager. All data processing and analysis was performed using ONI's online platform, CODI (https://alto.codi.bio).

Lateral Flow Strips. Nitrocellulose cards (HF135MC100) from Millipore Sigma were striped using a Kinematics Matrix 1600 dispenser (Grand Rapids, MI). For the EV capture zone, anti-CD9 (9PU), anti-CD63 (63PU), and anti-CD81(81PU) antibodies from Immunostep (Salamanca, Spain) were mixed at 0.5 mg/mL concentration and dispensed at 2 μL/cm. Mouse monoclonal anti-p24 C01655 M from Meridian Bioscience (Cincinnati, OH) was striped at 1 mg/mL concentration at 2 μL/cm. For the control line, anti-mouse IgG M8890 from Sigma-Aldrich was striped at 0.5 mg/mL at 2 μL/cm.

Conjugates. Mouse monoclonal anti-p24 C01653 M from Meridian Bioscience was conjugated to Estapor Red Intense microbeads (300 μm) following the manufacturer's instructions from Millipore Sigma. Rabbit monoclonal anti-Nef R0026 from Intuitive Biosciences was conjugated to Estapor Blue Intense microbeads (300 μm) following the manufacturer's instructions from Millipore Sigma. For the full prototype strips, glass fiber conjugate pads (GFDX, Millipore Sigma) were soaked with a 0.01 % solution of mixed red and blue conjugate beads and allowed to dry overnight.

Lysis Buffer. Lysis Buffer was 2 mM Tris-HCl, 0.1 % NP-40, 0.1 % sodium deoxycholate, 0.01 % SDS, 9 mM HEPES, 150 mM NaCl, 0.045 % Tween 20, 0.9 % BSA, and 0.1 % Saponin.

Sample Buffer. 2 % BSA with 5 mg/mL mouse IgG I5381 (Millipore Sigma).

Lateral Flow Assay and Analysis. P24 single test line strip. For each plasma sample, 50 μL was slowly applied to the sample pad and allowed to run for 30 s. Then 125 μL of Lysis Buffer was added just

upstream of the sample pad. Each strip was allowed to develop for 3 min before analyzing. The signal intensity for each test and control strip was determined using an Axxin lateral flow strip reader (AXXIN AX-2X–S, Axxin, Fairfield Australia). Signal intensity, captured as peak height, was performed using the Kinetic Designer mode software. Values for peak intensity are shown as Arbitrary Units (A.U.).

P24 and Nef dual test line strip. Dual target LFA strips used the same capture and detection reagents for p24 as the p24 alone strips. The anti-Nef capture antibody was a rabbit monoclonal anti-Nef (clone R0008), and the detection antibody was a rabbit monoclonal anti-Nef (clone R0026). Sample order was randomized and blinded. Plasma samples were tested in duplicate. 20 μL of 5 mg/mL murine gamma globulin (Rockland Immunochemicals) was added to each sample and incubated for 10 min to reduce nonspecific background signal. 70 μL of sample was slowly added to the strip and allowed to absorb for 1 min. After 1 min, 125 μL of Lysis Buffer was added to the strip and incubated for 45 min. The strip was then imaged on the Axxin Reader using a program designed to read both lines (p24 and Nef) simultaneously. Signal intensity, captured as peak height, was performed using the Kinetic Designer mode software. Values for peak intensity are shown as Arbitrary Units (A.U.).

Statistical Analysis. Statistical analysis was performed with GraphPad Prism (version 10.4.0, La Jolla, CA). Data was analyzed by performing a Welch's unpaired *t*-test or Mann-Whitney non-parametric test. P-values less than 0.1 (*), 0.01 (**), 0.001 (***), and 0.0001(****) were considered statistically different and are designated with asterisks as shown. Data were presented as the mean ± standard deviation.

3. Results

EVs enriched from HIV + volunteers and from HIV + cell lines contain HIV proteins

To confirm HIV biomarkers of interest we first selected a small set of plasma samples from volunteers of the placebo arm of the HVTN505 vaccine trial. Enrichment of EVs was performed for 30 samples (10 HIV-, 20 HIV+) by a resin-based method, followed by characterization of the resulting particles. Enriched particles were characterized for size and concentration by tunable resistance pulse sensing (TRPS). A brief overview of automated Western analysis and quantification to determine area under the curve (AUC) is found in Supplemental Fig. 1. Overall, there was no significant difference between the two groups of samples for total concentration of enriched EVs (Fig. 2A). Next, EVs were evaluated for a standard EV cargo protein, TSG101. Full Western images are available in Supplemental Fig. 2 and corresponding values associated with each band's signal intensity (Supplemental Table 1). TSG101 levels were compared by Western analysis to confirm that the EV enrichment process was successful and that there were similar levels between groups. As shown in Fig. 1B, TSG101 levels were equivalent between HIV- and HIV + sample sets demonstrating that the EV isolations and loading of the Western were equivalent between groups and samples.

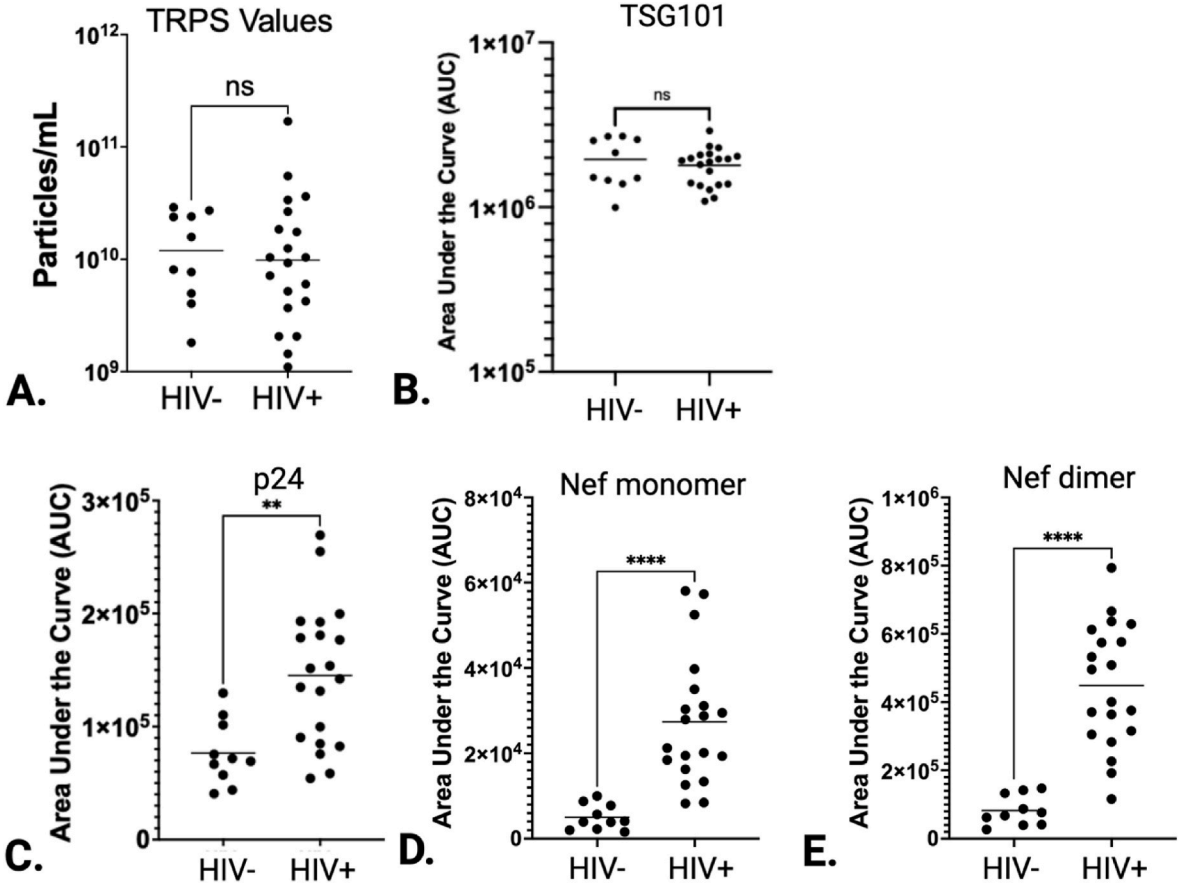

Fig. 1. Detection of EV markers and HIV proteins in EVs enriched from plasma. (A) TRPS analysis demonstrating equivalent particle size between HIV- and HIV + enriched EVs. **(B)** Western analysis demonstrating equivalent levels of TSG101 in 200 μg HIV- and HIV + enriched EVs quantified by Area Under the Curve (AUC). **(C)** Western analysis showing the detection of p24 in EVs enriched from HIV + individuals. **(D)** Western analysis showing the detection of Nef in EVs enriched from HIV + individuals. Values for the AUC of the Nef monomer at approximately 33 kDa shown. **(E)** Western analysis showing the detection of Nef dimer in EVs enriched from HIV + individuals. Values for the AUC of the Nef dimer at approximately 56 kDa shown. ** indicates a p-value <0.01, **** indicates a p-value <0.0001. "ns" indicates a p-value that is "not significant" or greater than 0.1. *Created in BioRender. Luke, K. (2025)* https://BioRender.com/i78c888.

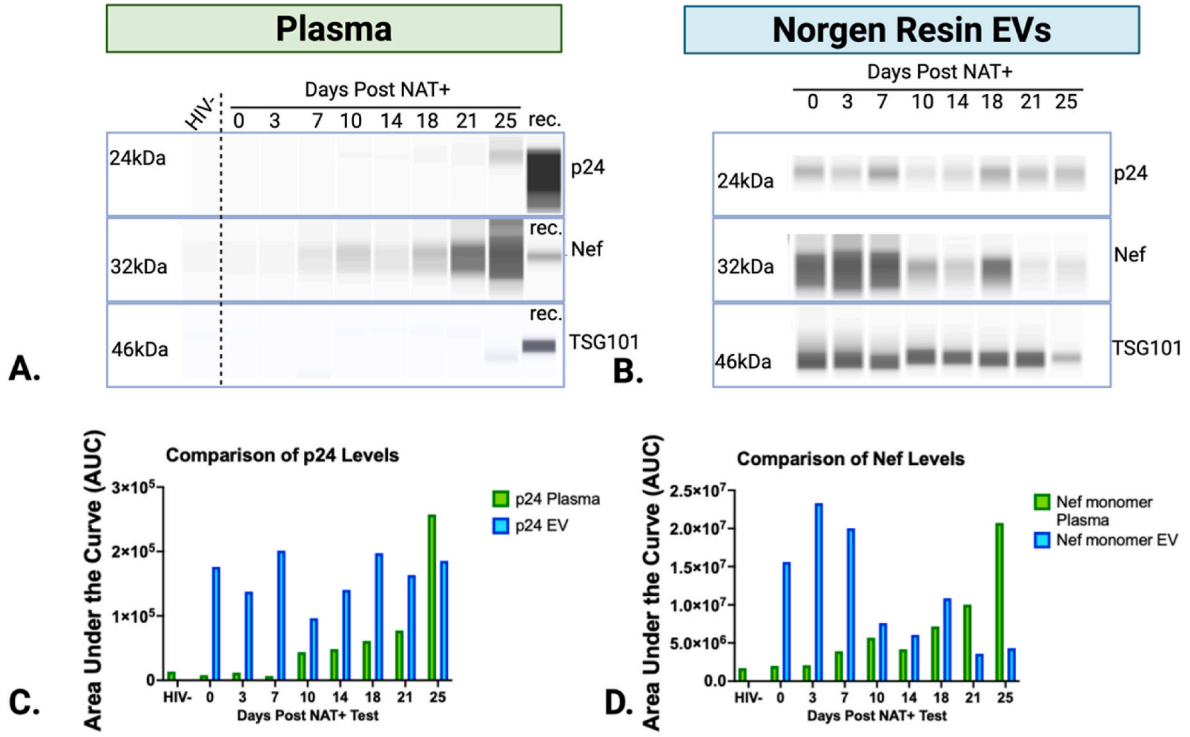

Fig. 2. Detection of HIV proteins in plasma and enriched EVs from an HIV positive individual over the course of infection. (A) Western analysis of approximately 4 μg of plasma for p24, Nef, and TSG101. Molecular weights determined from ladder run on same cartridge. Recombinant proteins are shown for reference. An HIV- "normal" human plasma sample is shown in the left column for reference. Time after first nucleic acid test (NAT) positive result corresponding to that sample is shown above each lane. **(B)** Western analysis of approximately 2–4 μg of resin enriched EVs for p24, Nef, and TSG101. Molecular weights determined from ladder run on same cartridge. **(C)** Comparison of AUC values for p24 from plasma versus EV for each sample. **(D)** Comparison of AUC values for Nef monomer from plasma versus EV for each sample. *Created in BioRender. Luke, K. (2025)* https://BioRender.com/ssr42iy.

Work by others has shown that HIV proteins including p24 and Nef have been observed *in vitro* in EVs in cells transfected with plasmids expressing these proteins, and *in vivo* in EVs of people living with HIV. Similarly, we observed p24 and Nef in enriched EVs from HIV + individuals. In Fig. 1C–E, there is a significant difference (p-value <0.01) in the mean AUC for p24 and Nef between groups. Both the monomeric and dimeric forms of Nef were quantified; the full Western is available in Supplemental Fig. 2C. The strongest signal is in the dimer form of Nef, which is not surprising as Nef dimers are critical for efficient viral replication.[22] Dimers are found both associated with membrane and cytosol, and homodimers can withstand the reducing conditions of Western assays as cysteine bonds are not involved in dimerization. This suggests that HIV proteins can be detected in EVs isolated from HIV + plasma samples and that Nef and p24 have potential to be used as target antigens for diagnostic purposes.

Because p24 is currently used in the 4th generation antigen/antibody laboratory-based tests as a marker of acute infection but is typically not present in plasma throughout the course of infection, the addition of Nef as a biomarker could be important to increasing the sensitivity of the antigen-only assay. To determine when HIV-EVs could be detected, EVs were isolated from a seroconversion panel drawn from a single volunteer. The seroconversion panel consisted of samples collected beginning on the date of the first positive nucleic acid-based laboratory test. Additional plasma samples were then collected periodically out to 25 days. The enriched EVs were compared to their paired source plasma using automated Western analysis methods to evaluate levels of TSG101, p24, and Nef.

In the plasma samples, equivalent amounts of protein (4 μg) were run for each sample. No appreciable bands for TSG101 were observed in the plasma samples, as expected from this marker of extracellular vesicles (Fig. 2A). Faint bands for p24 were observed by day 25 while Nef had faint bands starting at day 7 and increasing in signal in the later samples. A higher concentration of plasma was evaluated by Western to see if p24 and Nef were present but just below the limits of detection (Supplemental Fig. 3A). While p24 was not detected even at this significantly higher level of protein loaded, TSG101 was detected. This is likely due to EVs and multivesicular bodies present in plasma itself, which may be detected when loading significantly higher levels of total protein. It is important to note that even when loading large amounts of plasma, p24 was undetectable. Nef was detectable, whether from EVs present in the sample or from circulated Nef in plasma and highlights the utility of Nef as an additional biomarker of interest for HIV detection.

More significant is the abundance of p24 and Nef in EVs enriched from the early samples. As shown in Fig. 2B, levels of p24 and Nef are detectable in EVs from the first sample onward suggesting that the EV associated HIV antigens are present and detectable at the date when the volunteer first tested positive by a nucleic acid-based test. Similar levels of TSG101 are observed across samples (Fig. 2B), which is also reflected in the consistent protein concentration (Supplemental Fig. 4). Strong signal is seen in all plasma and EV samples, including the HIV- sample, from 50 to 66 kDa, obscuring the band for the Nef dimer and preventing a comparison of this isoform between plasma and EVs (Supplemental Fig. 4). However, the comparison of the monomer at approximately 30 kDa demonstrates that Nef can be detected in the earliest timepoints. The lower signal observed after 10 days may be specific to this sample and will be further investigated in larger sample sets.

Directly comparing the signal intensities of p24 and Nef in plasma and enriched EVs (Fig. 2C and D) demonstrates that EVs are enriched in p24 and Nef, and plasma EVs may be a unique reservoir for these biomarkers. While it is possible that this individual volunteer may not be representative of the spectrum of individuals living with HIV, these results, in conjunction with the results of the 20 additional HIV positive samples from Fig. 1 further supports the hypothesis that HIV-EV proteins are promising targets for development of a diagnostic test.

Tetraspanins can be used to capture EVs on lateral flow. Tetraspanin membrane proteins CD9, CD63, and CD81 are the most common EV-associated markers reported in the literature[23–25] and they have been used for EV capture in many studies, including studies using ELISA,[26,27] flow cytometry,[28] lab-on-a-chip assays,[29,30] and LFIA.[31,32] The feasibility of a research-grade lateral flow device to detect EVs using anti-CD9 and anti-CD81 as capture antibodies has been established.[32] To replicate this, a mix of anti-CD9/CD63/CD81 antibodies, all at 0.5 mg/mL, was striped on nitrocellulose strips which functioned as a capture zone. These strips were assembled with a wicking pad for a dip stick assay. Briefly, each strip was placed into a well with 50 µL of diluted EVs and was then transferred to a well with anti-CD63 gold conjugate to visualize EV capture on the anti-tetraspanin capture zone as shown in Fig. 3A. The EVs from A375 cells are considered an EV "standard" and are purified by ultracentrifugation followed by lyophilization and are slowly resuspended in water prior to use. As little as 0.5 µg of A375 EVs was detected in the EV capture zone when using a lateral flow strip reader (Fig. 3B). At the highest concentration of 40 µg the signal was strong but not saturated, which is not unexpected when capturing with a three antibody mix and detecting with just one of those antibodies. These results indicate a high binding capacity for capturing EVs in solution and confirmed that the anti-tetraspanin antibodies selected for this study successfully capture EVs in a lateral flow format.

Characterization of HIV + cell line expressing p24 and Nef. To develop the lateral flow test, well-characterized positive control material was required that contain p24 and Nef. The H9MN FI cell line described by Imamichi et al. was established from a single-cell clone of the H9MN T cell line that contains an intact full-length (8.9 kb) provirus encoding all open reading frames of HIV-1, and expressing p24 and Nef.[11] This cell line, along with the parental uninfected H9 cell line, was washed with PBS and grown in FBS-free media for 48 h to reduce bovine EV contamination. EVs were then enriched from the conditioned culture media by size exclusion chromatography (SEC), concentrated, and characterized. Enriched EVs were characterized for the presence of EV specific proteins TSG101 and the tetraspanin CD81, and for the HIV proteins of interest p24 and Nef. As shown by transmission electron microscopy (TEM) images of enriched EVs in Fig. 4A and F, the SEC enriched EVs display the classic cup-shaped morphology indicated by with arrows in each figure. These enriched EVs did have high amounts of protein, seen as the smaller particles in the field of view, which are likely albumin that was concentrated during the enrichment process. This was consistent between the two preparations. H9 EVs enriched from cell culture supernatants had particle counts with a mean diameter of 87 nm and 3×10^9 particles/mL while the EV enriched from the H9MN FI cells had a similar mean diameter of 91 nm and higher particle counts at 4×10^{10} particles/mL, as shown in Fig. 4B and H, respectively. In Fig. 4C, the H9 EVs demonstrated the presence of TSG101 and CD81 consistent as markers of EVs, and no detectable p24 or Nef as expected from uninfected cells. The EV enriched from H9MN FI cells, shown in Fig. 4I, also had bands for TSG101 and CD81 which is consistent with markers of EVs, as well as bands for p24 and Nef demonstrating expression of the HIV proteins required for the positive control material.

To further confirm that the HIV proteins p24 and Nef are associated with EVs, super resolution microscopy was performed on the SEC-enriched EVs. EVs were captured using a non-specific EV capture method with phosphotidylserine and stained with anti-tetraspanin trio (CD9/CD68/CD81), p24, and Nef. As shown in Fig. 4D (negative control) and J (H9MN FI), p24 and Nef are observed colocalized in permeabilized H9MN FI EVs with CD9/CD63/CD81 when captured on tetraspanin immunocapture surfaces. However, there was low signal with fewer than 2000 captured particles, so additional characterization of the SEC enriched EVs was performed with each antibody individually to optimize the conditions for microscopy using anti-p24 or anti-Nef, respectively. Individual tetraspanin composition was examined in EVs (Fig. 4E and K), and similar distribution of CD9, CD63, and CD81 was observed between H9 and H9MN FI SEC enriched EVs. There are some differences between the percentages of dual or triple positive EVs, but overall, the two cell lines express EVs with all three tetraspanins present.

Next, colocalization of p24 and Nef with tetraspanins were examined in H9 and H9MN FI enriched EVs. EVs were either treated with permeabilization buffer to allow antibodies to transit the membrane and stain internal cargo (permeabilized) or treated with PBS (unpermeabilized). In H9MN FI enriched EVs, p24 was observed in approximately 40 % of tetraspanin positive particles, compared to the background level of p24 staining in H9 enriched EVs at 4 % (Fig. 4L). Similarly, Nef was observed in approximately 19 % of permeabilized H9MN FI EVs, compared to the nonspecific background staining of 7 % in H9 EVs. Because other studies have reported Nef to be observed associated with the external EV membrane,[33] H9MN FI EVs were also stained without permeabilization. When compared to H9 unpermeabilized EVs, there was about 5 % increase in Nef events in H9MN FI EVs suggesting a small amount of externally associated Nef. An additional 7 % increase in Nef staining was observed in H9MN FI EVs by permeabilization, suggesting that there is Nef is present as cargo as well as associated with the external membrane. The values for the percent tetraspanin trio-stained events for each condition can be found in Supplemental Fig. 5. These

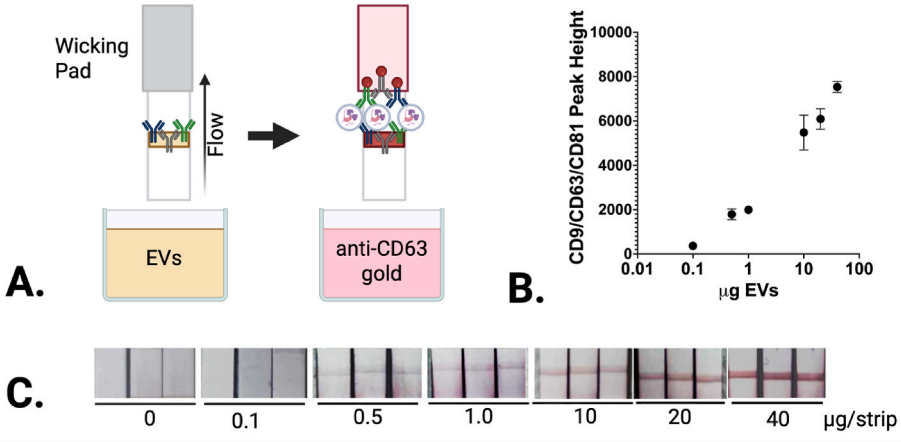

Fig. 3. EVs and can be detected in a lateral flow format. (A) Schematic of EV detection on lateral flow dip stick. Anti-tetraspanin antibodies striped onto nitrocellulose with a wicking pad placed into a well with diluted EVs. EVs flow up the strip and bind to the capture line. The strip is transferred to a well with an anti-CD63 gold conjugate to detect EVs. **(B)** Triplicate measurements of peak heights for each dilution of A375 EVs are graphed with standard deviations. **(C)** Images of triplicate strips of purified EVs detected with an anti-CD9 gold conjugate to determine the visual LOD of detection. *Created in BioRender. Luke, K. (2025)* https://BioRender.com/e70p646.

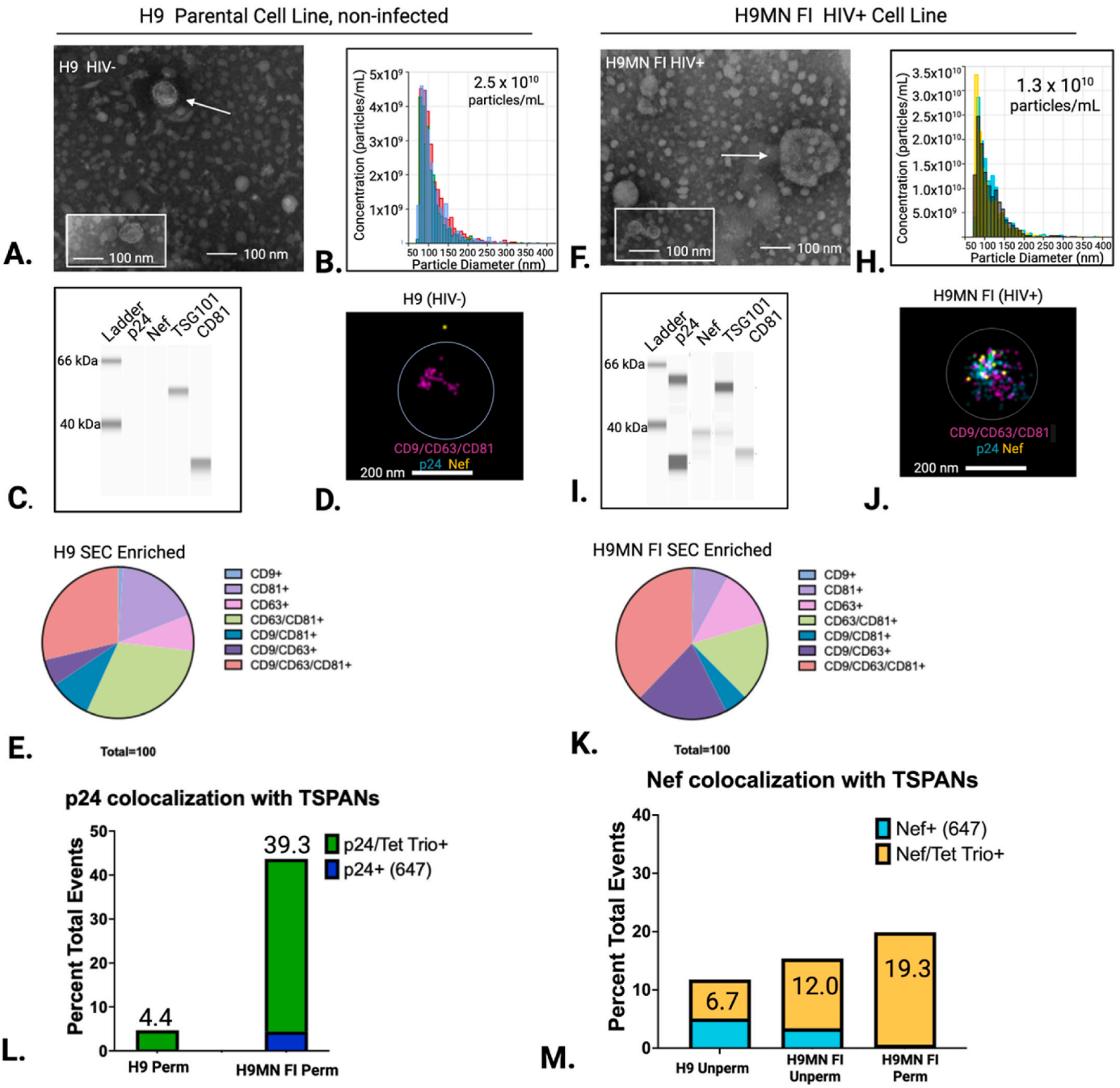

Fig. 4. Characterization of p24 and Nef from H9MN FI EVs. (A–E) Figures correspond to EVs enriched from H9, parental HIV- cell lines. **(F–K)** Figures correspond to EVs enriched from H9MN FI (HIV+) cells. **(A, F)** TEM images of SEC enriched EV with a 100 nm bar for sizing. Inset highlights interesting EVs. **(B, H)** TRPS analysis of EVs enriched from H9 and H9MN FI cells, evaluating particle size on the x-axis and concentration on the y-axis. **(C, I)** EVs enriched by SEC from H9 and H9MN FI cells were tested on an automated Western analysis system for the presence of HIV proteins Nef and p24, and EV proteins CD81 and TSG101. **(D, J)** Image of a representative "cluster" from super resolution microscopy analysis of EVs enriched from H9 and H9MN FI cells evaluated for presence of two HIV proteins using antibodies conjugated to dSTORM-compatible fluorophores, p24 in blue, Nef in yellow, and a pan-tetraspanin (mix of anti-CD9, CD81 and CD63) in pink. A 200 nm bar is shown for scale in each panel. **(E, K)** Super resolution microscopy evaluation of individual tetraspanin expression using anti-CD81 (647 emission), anti-CD63 (561 emission) and anti-CD9 (488 emission) on EVs enriched from H9 and H9MN FI cells. Percents of individual, dual, and triple positive EVs graphed in a pie chart from the mean of total counted clusters in triplicate lanes. **(L)** Super resolution microscopy evaluation of combined tetraspanin expression using anti-CD81/anti-CD63/anti-CD9 (561emission) and p24 (647 emission) on EV enriched from H9 and H9MN FI. Percents p24 single positive events graphed in blue, tetraspanin trio/p24 dual positive events graphed in green. Events are graphed in a bar chart from the means of total counted clusters of triplicate lanes. **(M)** Super resolution microscopy evaluation of combined tetraspanin expression using anti-CD81/anti-CD63/anti-CD9 (561emission) and Nef (647 emission) on EV enriched from H9 and H9MN FI cells. Percents Nef single positive events graphed in teal, tetraspanin trio/Nef dual positive events graphed in orange. Events are graphed in a bar chart from the means of total counted clusters of triplicate lanes. *Created in BioRender. Luke, K. (2025)* https://BioRender.com/u67bxq3.

data confirm that EVs enriched from H9MN FI cells contain HIV proteins including p24 and Nef and are suitable controls to be used in further analysis.

HIV-EV cargo can be detected on lateral flow. A two-stage lateral flow assay was designed around the concept of separating and capturing EVs from an input sample in the first stage, then lysing the EV membrane to release cargo proteins for detection upstream in the second stage, as shown in Fig. 5A. This is beneficial because the EV cargo proteins are free from host derived interfering IgG present in plasma, which avoids antigen/antibody complexes from seropositive samples that can interfere with detection.

First, sample is added to the sample pad and flows up the lateral flow strip to the first stage where EVs are captured by the anti-tetraspanin line. If the sample is whole blood, the sample pad may contain additives to retain red blood cells in the sample pad to permit plasma to flow past. Since HIV virus particles may also contain tetraspanin transmembrane proteins, they could be captured on the EV capture line as well. Next, an EV lysis buffer is added to the EV capture zone, perforating the EV membrane to release EV cargo. As shown in Fig. 5A, there are 3 possible sources of p24: from the virus particle, from EVs, or free in the plasma. The liberated proteins migrate up the strip to the conjugate pad and interact with the anti-p24 conjugate. Antigen-conjugate complexes then flow to the second stage where they can be captured at the test line. Any remaining free conjugate is captured at the control line.

Because p24 is currently included on antigen/antibody rapid tests, there are well-validated antibody pairs available for use with lateral flow. No compatible antibody pairs were found for Nef that could be used with lateral flow (data not shown), so p24 was used as a single test line to perform proof-of-concept experiments in the novel two-stage EV-based lateral flow assay while the immunization of rabbits for rabbit monoclonal antibody development against Nef was performed.

Using human plasma as the sample diluent, increasing amounts of purified H9 or H9MN FI EVs were spiked into a 50 µL sample volume and run on the prototype two-stage lateral flow strips. The human plasma used was not treated to remove EVs or other vesicles, the p24-containing EVs were added in addition to the exogenous EVs in the plasma. After a brief 30 s incubation to allow EVs to bind to the EV capture zone, 125 µL of Lysis Buffer was pipetted just past the sample pad and flowed up the EV capture zone to perforate the EV membranes, release cargo, and push that cargo through the conjugate pad. As shown in Fig. 5B, the addition of Lysis Buffer significantly increases the signal at the test line when compared to PBS, which contains no lysis reagents. This suggests that

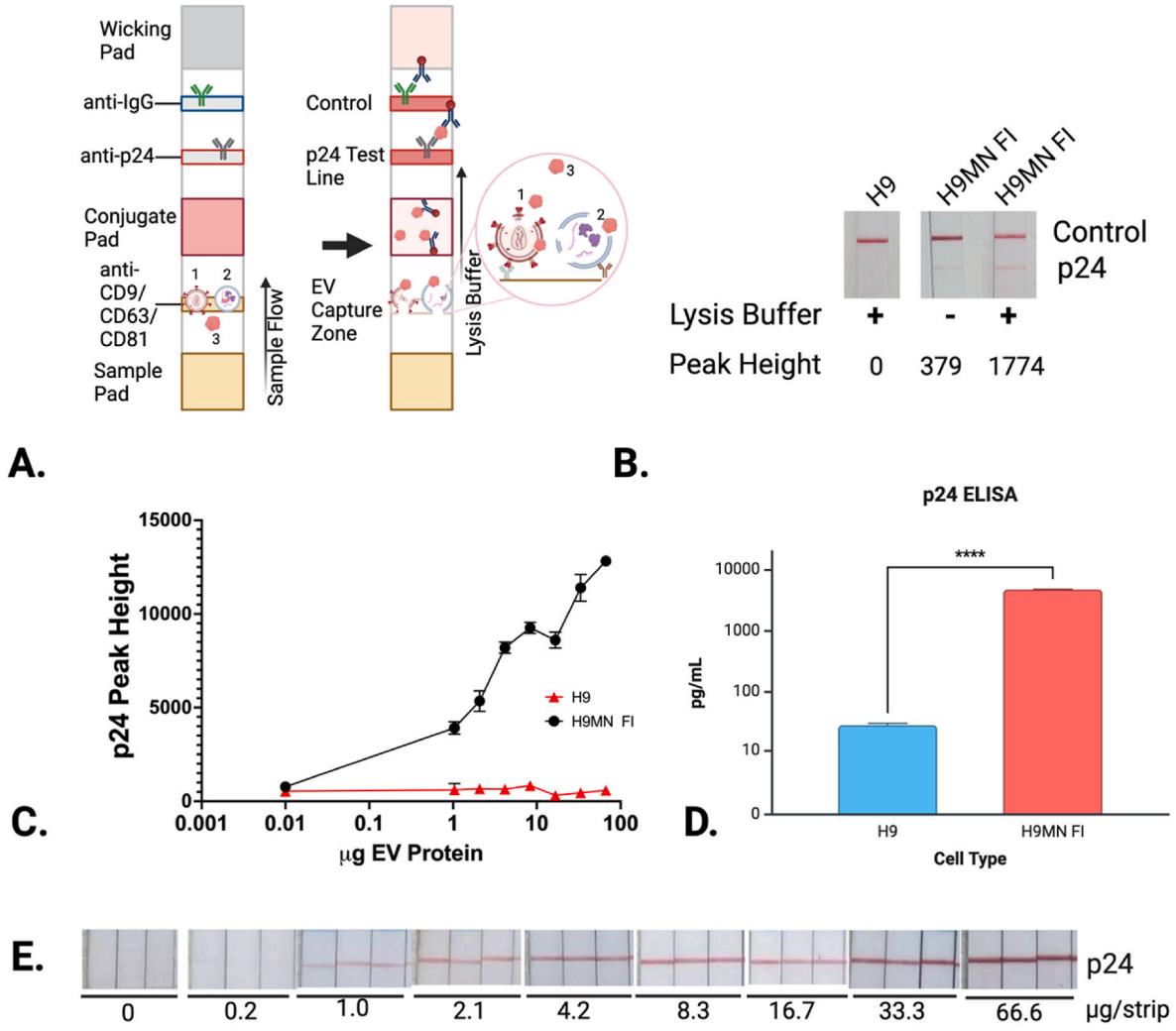

Fig. 5. Detection of p24 from HIV-EVs by lateral flow. (A) Schematic of the two-stage lateral flow design that includes an EV capture zone and a test zone. Inset shows three distinct sources of p24 protein: 1) p24 from HIV virus particles, 2) p24 from HIV-EVs, and 3) plasma p24. **(B)** Comparison of p24 detection from EVs enriched from H9 and H9MN FI cells with and without Lysis Buffer, as indicated below each image. **(C)** Peak heights of the p24 test line signal intensity captured by an Axxin reader. Triplicate measurements of each dilution of enriched EVs from H9 (HIV-) or H9MN FI (HIV+) cells spiked into human plasma. Error bars represent standard deviations from the mean. The x-axis shows the amount of EV protein added to each strip. **(D)** Mean p24 values from 3 µg of H9 or H9MN FI EVs after treatment with Lysis Buffer. **(E)** Images of the test line from the triplicate lateral flow strips. *Created in BioRender. Luke, K. (2025)* https://BioRender.com/f20z850.

the release of p24 from 20 µg of H9MN FI EVs is enhanced by addition of a buffer that will lyse membranes. Several potential formulations for lysis buffer were tested (data not shown) and are the subject of another manuscript in progress. This work supports the data shown in Fig. 5 that p24 levels increase upon permeabilization of the EV membrane.

Next, HIV-EVs were used to test the limit of detection of the two stage lateral flow strips. This work was performed on the p24-only test line strips. Briefly, EVs enriched from H9MN FI and H9 cells were diluted in healthy HIV- human plasma to create an 8-point standard curve and tested in triplicate. Images of the p24 test line were captured and mean peak height of the test line from triplicate strips was measured in arbitrary units (AU) as shown in Fig. 5C. Visual detection of p24 was possible down to 1 µg of H9MN FI EVs (2.93×10^8 particles) spiked into human plasma, as seen in Fig. 5E. That visual LOD corresponds to approximately 750 pg/mL of p24 when extrapolated from the 3 µg sample measured by a commercial p24 ELISA (Fig. 5D). The only source of p24 in this sample is from the EVs spiked into the human plasma. Despite competition with the endogenous non-HIV-EVs for binding to the EV capture zone, p24 detection was possible, which supports the feasibility of this design.

After selection of a pair of rabbit monoclonal antibodies to recombinant Nef, integration of the second test line was performed using a second color conjugate. As shown in Fig. 6A, the only change to the configuration was, the addition of the anti-Nef test line and the anti-Nef Blue conjugate to the conjugate pad. Briefly, the LOD for p24 (Test Line 1) and Nef (Test Line 2) on the strip was determined by mixing the recombinant proteins together in Sample Buffer and performing a serial dilution. Five replicates per concentration were tested. A total of 50 µL of

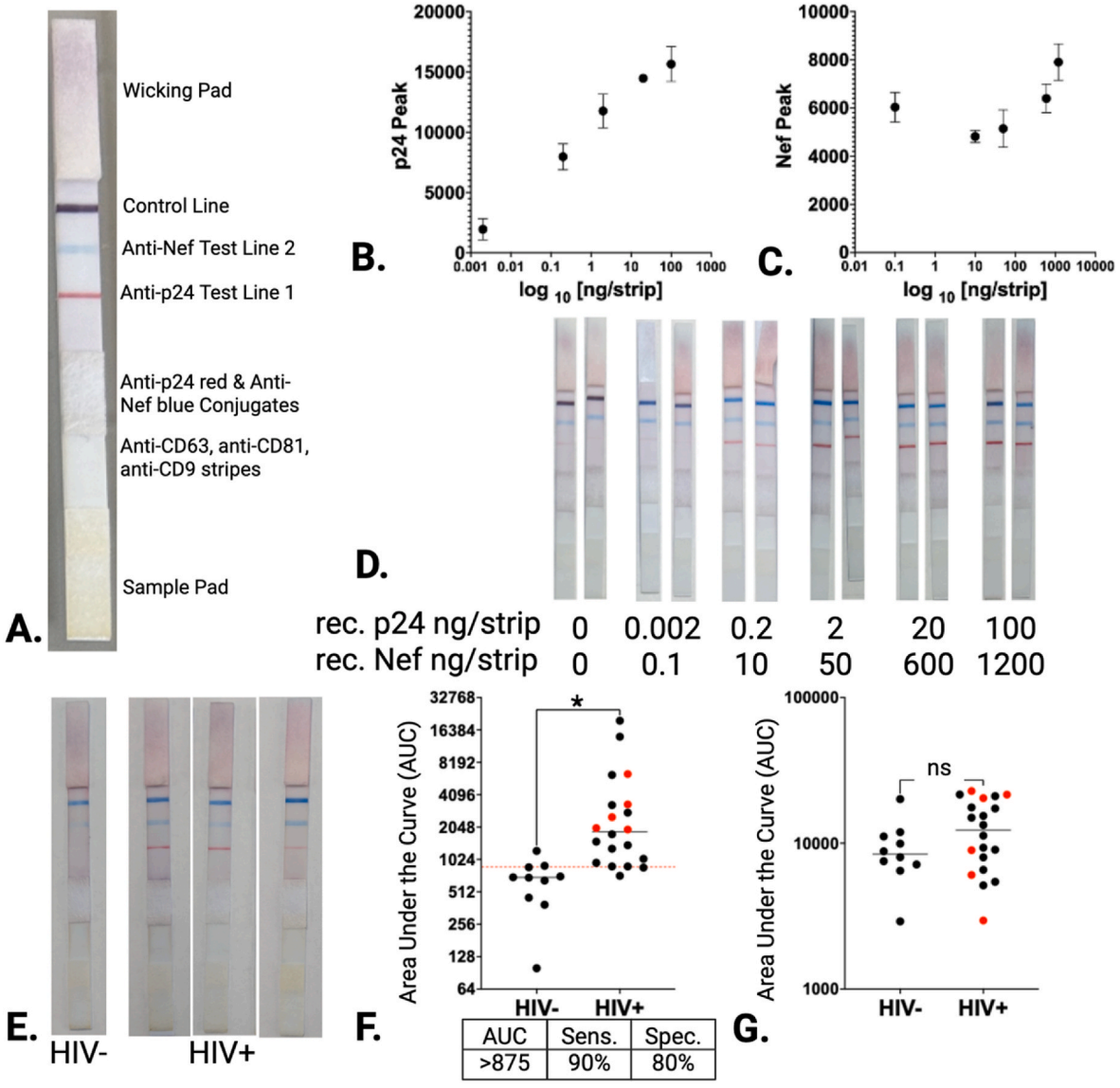

Fig. 6. Plasma Samples Tested on Prototype Lateral Flow Tests. (A) Labelled image of the two-stage lateral flow prototype with an EV capture zone and a test zone that includes both the p24 and the Nef test line. **(B)** Results from the limit of detection analysis of mixed recombinant protein in buffer. Measurement of the intensity of the p24 test line. **(C)** Results from the limit of detection analysis of mixed recombinant protein in buffer. Measurement of the intensity of the Nef test line. (**D**) Representative images of the mixed recombinant proteins used to calculate results for B and C. (**E**) Images of the prototype test strips with a representative HIV- and HIV + plasma samples. (**F**) P24 test line AUC values from 10 HIV- and 20 HIV + plasma samples. The red dotted line represents the cut-off value determined by ROC analysis, the value is shown below the graph at 90 % Sensitivity and 80 % Specificity. HIV + specimens graphed in black were those under ARV treatment. Those in red indicate no ARV treatment. * represents statistical significance at a p-value less than 0.1. (**G**) Nef test line AUC values from 10 HIV- and 20 HIV + plasma samples. HIV + specimens graphed in black were those under ARV treatment. Those in red indicate no ARV treatment. *Created in BioRender. Luke, K. (2025)* https://BioRender.com/220tmf9.

diluted recombinant antigen was added to the strips and allowed to flow for roughly 30 s before adding 55 μL of Lysis Buffer. Strips were imaged and analyzed on the Axxin reader to obtain a quantitative value for the band signal intensity, graphed as mean peak height in arbitrary units (AU). As shown in Fig. 6B, the LOD for p24 in the full prototype strip is 0.2 ng/strip. The LOD for Nef (Fig. 6C) was determined to be 150 ng/strip, with high background signal noted at lower concentrations. This non-specific binding was observed with the buffer only control and was a considerable issue in the optimization of this prototype assay. Images of duplicate strips for each dilution are shown in Fig. 6D. The Sample Buffer did include mouse IgG as an additional blocking reagent to reduce nonspecific binding of the blue rabbit anti-Nef conjugate to the mouse anti-p24 test line, but some binding was still observed even in buffer alone. Despite testing several types of blocking reagents (data not shown), no significant reduction in the non-specific binding was observed in the Nef test line, which resulted in high background signal with the blue conjugate.

Last, the set of 30 plasma samples were tested on the full prototype strips. To address the nonspecific binding observed in the LOD experiments,20 μL mouse IgG was added to 50 μL of plasma sample and incubated for 10 min prior to adding to the sample pad. The resulting 70 μL volume was then slowly pipetted onto the sample pad and allowed to migrate across the EV capture zone for 60 s, followed by addition of 125 μL of Lysis Buffer to the sample pad by dropwise addition. The sample was allowed to migrate for a total of 45 min before imaging on the Axxin reader, where values were acquired for the Test Line 1 (T1) corresponding to p24 and for Test Line 2 (T2) corresponding to Nef. Some representative images of plasma samples on the prototype strips are shown in Fig. 6E, with the full quantified values for each test line graphed for p24 and Nef in Fig. 6F and G, respectively. Images for all strips and tables with the corresponding test line values are available in Supplemental Fig. 6. The values for the p24 test line were significantly different between the HIV- and HIV + group and had a Sensitivity of 90 % and Specificity of 80 % by ROC analysis. The background observed in the Nef test line resulted in no significant difference between the two groups. The level of nonspecific binding by the detection antibody was too high to distinguish any specific signal. Despite only having results from the p24 test line, this prototype assay had 90 % with a small sample set. This highlights the potential for this assay and emphasizes the need for further development of the Nef antibodies as reagents.

4. Discussion

Improving at-home HIV testing by making an antigen-only test will require more than just improving the sensitivity of the currently available p24 antigen test. The capsid protein was among the first targets for antigen-based HIV assays as it is the most abundant protein produced by the virus, and it is present throughout infection, even in individuals on ART. However, levels of p24 decrease after the initial rise, requiring another constitutively expressed protein like Nef to be included in the assay for detection after p24 expression wanes. Although p24 is a component of combination antibody/antigen tests, our previous work, along with decades of literature, suggest that using p24 alone does not provide sufficient sensitivity and specificity. In addition, the emergence of an antibody response corresponds with a steady decline in detectable p24—eventually to levels below the LOD of the current assay—likely due to the formation of antigen-antibody complexes in the blood.[34] The development of an EV-based lateral flow test for p24, with its well-validated set of reagents, was the most reasonable path to pursue to demonstrate proof-of-concept while developing immunoreagents for other promising targets like Nef. The results presented here evaluated cargo proteins from EVs enriched from plasma donated by people living with HIV. The HIV proteins p24 and Nef were confirmed as potential biomarkers present in enriched EVs (Fig. 1). Admittedly, the resin-based method of EV enrichment used in this study does not produce high purity EVs but was selected as an early screening method for use with limited sample volumes. Because we are not attempting to create a pure EV population, and do not intend to for the final diagnostic product, we acknowledge that the source of the HIV proteins could be from EVs, protein contaminants, HIV virus particles, or other vesicular bodies. Whole blood that contains these types of vesicles and particles will be the input sample for the diagnostic, and as the title of this paper suggests, the diagnostic design seeks to utilize these similarities to increase the sensitivity of the test. The intention was to enrich those particles that contain the HIV proteins of interest to characterize them, rather than purify EVs exclusively. While the specific serological location of the antigens is an interesting biological question to pursue, it is not essential to the development of this EV-based diagnostic for HIV.

In Fig. 1A and B, both HIV- and HIV + groups had no statistical difference in overall particle counts andTSG101 levels. Previous reports in the literature have shown elevated levels of EVs from HIV + plasma[10]; however, the samples in this study were remnants from a vaccine study and may differ in collection method, storage method, age of samples, and stage of infection for the HIV + volunteers. Given the age of the samples that were collected from 2010 to 2013 and EV enriched in 2024, it is reasonable to assume that there could be variability in the resulting EVs that could obscure any differences in overall particle counts. However, this should not affect the overall goal of the assay. If HIV biomarkers can be detected in remnant samples collected over 10 years ago in which EVs may be degraded, they should be more easily detected in fresh samples with no EV degradation.

Detection of p24 and Nef in EVs enriched from the plasma of HIV + volunteers confirmed that these were biomarkers to pursue as shown in Fig. 1C–E. Significant differences in the area under the curve (AUC) of the p24 and Nef bands were shown between groups. Values are shown for both the monomer and dimer form of Nef, which can be better viewed in the supplemental data (Supplemental Fig. 2C). Nef was observed both in its monomeric form as a weak band at around 27 kDa and as a dimer around 54 kDa. The addition of Nef as an HIV biomarker along with p24 demonstrates that EVs are a useful source of abundant HIV antigens in this set of samples. However, this set of samples was collected approximately 12 weeks after the initial positive nucleic acid test and does not cover the acute phase of infection. To address this, a commercial seroconversion panel was tested. This panel follows a single HIV + volunteer from the day that they first tested HIV + by a nucleic acid test; this is the most sensitive type of laboratory testing available and provides the earliest time point. A series of plasma samples are collected and tested with several FDA-approved diagnostics that include a p24 antigen ELISA, a laboratory-based antigen/antibody (Ag/Ab) test, and the antibody only at-home test. EVs isolated from this seroconversion panel was used to evaluate the presence of p24 and Nef in EVs in early HIV + samples that had known signal-to-cutoff values from the p24 antigen ELISA values and the Ag/Ab test, providing samples in which we expect detection of p24. Since Nef is not an antigen that is measured in these tests, our detection of Nef in Fig. 2A is interesting in relation to the timing and abundance of p24. As p24 tests are currently available, it is logical to assume that if detection of Nef by Western is possible at earlier timepoints and with more abundance, it should translate to detection in a diagnostic test that can at least obtain the sensitivity of the p24 test.

The timing of HIV antigen expression was investigated in this seroconversion panel. Both p24 and Nef were detectable in enriched EVs (Fig. 2B) beginning with the first sample, the earliest time point. This is notable because p24 and Nef are detected with higher signals in EVs compared to plasma up through the first 18 days (Fig. 2C and D). Our results suggest that addition of Nef as a biomarker for a protein-based diagnostic could have the potential to approach the sensitivity of a NAT test for early detection. These results are consistent with the studies from Kim et al. that demonstrated that HIV-EVs were released prior to viral release.[35] This will need to be further investigated with larger sample sets to confirm these results.

Nef is integral for viral infection and modulates intracellular

trafficking, which in turn enhances HIV persistence and disease acceleration.[36–38] Like p24, Nef appears very early in the disease course and is present at high concentrations (i.e., 10 ng/mL) in EVs in HIV-positive individuals, even when there are low levels of free circulating Nef.[39] Immunofluorescence data demonstrate the colocalization of Nef and the EV markers CD63 and CD81 in EVs derived from cultured human (Fig. 4C) and simian cell lines.[7,36] Similar studies using Western blot analysis demonstrate the colocalization of Nef, CD63, and CD81 in EVs.[7,10] A recent study by Vanpouille found a significant amount of Nef associated with the external surface of EVs which will be important to consider in future work when integrating Nef into the final design of the lateral flow test.[33] Our data, along with these studies showing Nef as an EV-based biomarker of HIV infection, support the addition of this antigen to a lateral-flow based antigen test.

Prior work by Oliveira-Rodríguez et al. demonstrated the potential to capture EVs from cell culture conditioned media and from biological specimens,[31] which we confirmed here with purified EVs (Fig. 3). In this system, detection of EVs is visible using less than 0.5 μg of EVs, which supports the concept of utilizing EVs to concentrate cargo proteins for downstream detection in a two-stage lateral flow assay. Later experiments (Fig. 5B and data not shown) evaluated different components and formulations of lysis buffer to both perforate the EV membrane to release the contents for interaction with the detection antibodies, and to physically chase the antigen/antibody complexes to the test zone. Further work is needed to optimize these components to balance antibody conjugate compatibility with membrane disruption potential.

EVs were enriched from a cell line with a full proviral genome that encodes all the open reading frames of HIV-1, simulating an infection in T cells. These EVs were spiked into human plasma, which contains approximately 10^9 EV particles/mL of heterogenous cellular origin. The limit of detection for EV-based p24 was then evaluated in these samples with the p24-only single test line lateral-flow assay. The anti-p24 capture antibody was printed onto lateral flow strips and an anti-p24 detection conjugate was dried onto the conjugate pad. The EV-spiked plasma samples were combined with sample buffer and added to the sample pad to flow up the EV capture zone. Lysis Buffer was added to the sample pad to release EV cargo from the captured EVs and move that cargo through the conjugate pad, allowing the conjugate and protein to interact. Flow continued through the anti-p24 capture line and the control line. EV-based p24 was detected on the lateral flow strips down to 1 μg of spiked H9MN FI EVs per strip (Fig. 5E). This supports the possibility of detection of HIV proteins associated with EVs on a lateral flow assay and demonstrates that the addition of Lysis Buffer results in better detection of the target HIV proteins from enriched EVs.

A pair of rabbit monoclonal antibodies were identified that could detect recombinant Nef, and they were added to the two-stage lateral flow assay. By conjugating the antibody to a blue bead and printing a second test line, the multi-antigen test zone could distinguish between p24 and Nef as shown in Fig. 6A. High background and non-specific binding with the rabbit anti-Nef antibodies prohibited measurement of Nef in the HIV + plasma samples during the small-scale evaluation of the prototypes. However, the p24 assay functioned well, with 90 % Sensitivity and 80 % Specificity. In this small sample set, the majority of the HIV + samples were collected from volunteers who were taking antiretroviral drugs (ARV) at some point during the original study (Fig. 6F and G). This was not a factor directly studied in these experiments as the sample collection timing did not correlate to the initiation of ARV timing. It will be considered for future studies, as some research has shown that ARVs can alter the contents of EVs secreted from HIV-1 infected cells.[40]

These studies were performed in prototype format, without any external housing or cassette. The ideal sample is a finger stick droplet of whole blood, to enable self-testing at home. This will require optimization of the sample pad for red blood cell exclusion, optimization of the EV capture zone to maximize the binding of EVs to capture as many HIV-EVs as possible and design modifications for an easy-to-use format for the at-home tester. With additional improvements like an outer housing for better sample flow, and rigorous testing of blocking and lysis buffers, the accuracy of this assay can be improved.[41] Work is currently underway to screen additional monoclonal antibodies against Nef, and to make recombinant chimeric antibodies with a murine immunoglobulin for better compatibility with lateral flow assays.

Overall, this work demonstrates a novel design of a two-stage lateral flow assay for capture of extracellular vesicles containing tetraspanins to concentrate EVs and a second nitrocellulose zone for detection of HIV target antigens. This is the first example, to our knowledge, of a potential at-home test method using extracellular vesicles to detect cargo proteins as diagnostic targets. As the title suggests, the design of this test utilizes the features shared between HIV and EVs to concentrate the biomarkers of interest. Addition of a lysis buffer to disrupt the EV membrane may also help dissociate any protein interactions that sequester antigen targets, further promoting detection. While these preliminary data demonstrate the feasibility of the design, there is additional work underway to optimize the antibodies to improve the performance of Nef in the assay. Ongoing studies are testing methods for separating whole blood on the sample pad and determining the minimal sample volume necessary to achieve the required sensitivity. The goal is to develop an at-home test for HIV that can detect infection sooner after risk events and potentially monitor for disease recurrence for those on ART or other therapeutic treatments.

CRediT authorship contribution statement

Casey Scott-Weathers: Writing – review & editing, Writing – original draft, Supervision, Methodology, Investigation, Formal analysis, Data curation, Conceptualization. **Kaitlyn King:** Methodology, Investigation. **Gary Baisa:** Writing – review & editing, Validation, Methodology. **John Hural:** Writing – review & editing, Resources, Data curation. **Kimberly Luke:** Writing – review & editing, Writing – original draft, Visualization, Supervision, Resources, Project administration, Funding acquisition, Formal analysis, Data curation, Conceptualization.

Declaration of competing interest

The authors declare the following financial interests/personal relationships which may be considered as potential competing interests: Kimberly Luke reports a relationship with Boost Biopharma that includes: equity or stocks. Casey Scott-Weathers reports a relationship with Boost BioPharma that includes: equity or stocks. Gary Baisa reports a relationship with Boost BioPharma that includes: equity or stocks. Kimberly Luke has patent #PCT/US2024/035613 pending to Intuitive Biosciences. If there are other authors, they declare that they have no known competing financial interests or personal relationships that could have appeared to influence the work reported in this paper.

Acknowledgements

This study was supported in part by the NIH NIAID contract 75N93023C00007. This study was made possible by samples provided by the HVTN (NCT00865566) as part of HVTN auxiliary study number 270-EXS_Luke_505. Figures were made in Biorender.com.

Appendix A. Supplementary data

Supplementary data to this article can be found online at https://doi.org/10.1016/j.vesic.2025.100084.

References

1. Nolte-'t Hoen E, et al. Extracellular vesicles and viruses: are they close relatives? *Proc Natl Acad Sci U S A*. 2016;113(33):9155–9161.

2. Ruiz-Mateos E, et al. CD63 is not required for production of infectious human immunodeficiency virus type 1 in human macrophages. *J Virol*. 2008;82(10):4751–4761.
3. Chertova E, et al. Proteomic and biochemical analysis of purified human immunodeficiency virus type 1 produced from infected monocyte-derived macrophages. *J Virol*. 2006;80(18):9039–9052.
4. Deneka M, et al. In macrophages, HIV-1 assembles into an intracellular plasma membrane domain containing the tetraspanins CD81, CD9, and CD53. *J Cell Biol*. 2007;177(2):329–341.
5. Booth AM, et al. Exosomes and HIV Gag bud from endosome-like domains of the T cell plasma membrane. *J Cell Biol*. 2006;172(6):923–935.
6. Campbell TD, et al. HIV-1 Nef protein is secreted into vesicles that can fuse with target cells and virions. *Ethn Dis*. 2008;18(2 suppl 2). S2-14-9.
7. Lenassi M, et al. HIV Nef is secreted in exosomes and triggers apoptosis in bystander CD4+ T cells. *Traffic*. 2010;11(1):110–122.
8. Ali A, et al. HIV-1 Tat: an update on transcriptional and non-transcriptional functions. *Biochimie*. 2021;190:24–35.
9. Ferdin J, et al. Viral protein Nef is detected in plasma of half of HIV-infected adults with undetectable plasma HIV RNA. *PLoS One*. 2018;13(1), e0191613.
10. Lee JH, et al. HIV-Nef and ADAM17-containing plasma extracellular vesicles induce and correlate with immune pathogenesis in chronic HIV infection. *EBioMedicine*. 2016;6:103–113.
11. Imamichi H, et al. Defective HIV-1 proviruses produce viral proteins. *Proc Natl Acad Sci U S A*. 2020;117(7):3704–3710.
12. Kornfeld H, et al. Lymphocyte activation by HIV-1 envelope glycoprotein. *Nature*. 1988;335(6189):445–448.
13. Clauss M, et al. Viral bad news sent by EVAIL. *Viruses*. 2021;13(6).
14. Aqil M, et al. The HIV Nef protein modulates cellular and exosomal miRNA profiles in human monocytic cells. *J Extracell Vesicles*. 2014;3.
15. Aqil M, et al. Transcriptomic analysis of mRNAs in human monocytic cells expressing the HIV-1 Nef protein and their exosomes. *BioMed Res Int*. 2015;2015, 492395.
16. Khan MB, et al. Nef exosomes isolated from the plasma of individuals with HIV-associated dementia (HAD) can induce Aβ(1-42) secretion in SH-SY5Y neural cells. *J Neurovirol*. 2016;22(2):179–190.
17. Anyanwu SI, et al. Detection of HIV-1 and human proteins in urinary extracellular vesicles from HIV+ patients. *Adv Virol*. 2018;2018, 7863412.
18. Technologies, O., OraQuick Advance Package Insert.
19. Huynh K, Kahwaji CI. *HIV Testing, in StatPearls*. 2025. Treasure Island (FL).
20. Miedouge M, et al. Analytical sensitivity of four HIV combined antigen/antibody assays using the p24 WHO standard. *J Clin Virol*. 2011;50(1):57–60.
21. Sundström C, Nilsson K. Establishment and characterization of a human histiocytic lymphoma cell line (U-937). *Int J Cancer*. 1976;17(5):565–577.
22. Poe JA, Smithgall TE. HIV-1 Nef dimerization is required for Nef-mediated receptor downregulation and viral replication. *J Mol Biol*. 2009;394(2):329–342.
23. Mathivanan S, Ji H, Simpson RJ. Exosomes: extracellular organelles important in intercellular communication. *J Proteonomics*. 2010;73(10):1907–1920.
24. Kowal J, et al. Proteomic comparison defines novel markers to characterize heterogeneous populations of extracellular vesicle subtypes. *Proc Natl Acad Sci U S A*. 2016;113(8):E968–E977.
25. Jolly C, Sattentau QJ. Human immunodeficiency virus type 1 assembly, budding, and cell-cell spread in T cells take place in tetraspanin-enriched plasma membrane domains. *J Virol*. 2007;81(15):7873–7884.
26. Logozzi M, et al. High levels of exosomes expressing CD63 and caveolin-1 in plasma of melanoma patients. *PLoS One*. 2009;4(4), e5219.
27. Duijvesz D, et al. Immuno-based detection of extracellular vesicles in urine as diagnostic marker for prostate cancer. *Int J Cancer*. 2015;137(12):2869–2878.
28. Campos-Silva C, et al. High sensitivity detection of extracellular vesicles immune-captured from urine by conventional flow cytometry. *Sci Rep*. 2019;9(1):2042.
29. Zhou S, et al. Integrated microfluidic device for accurate extracellular vesicle quantification and protein markers analysis directly from human whole blood. *Anal Chem*. 2020;92(1):1574–1581.
30. Chen YS, et al. An integrated microfluidic system for on-chip enrichment and quantification of circulating extracellular vesicles from whole blood. *Lab Chip*. 2019;19(19):3305–3315.
31. Oliveira-Rodriguez M, et al. Development of a rapid lateral flow immunoassay test for detection of exosomes previously enriched from cell culture medium and body fluids. *J Extracell Vesicles*. 2016;5, 31803.
32. Oliveira-Rodriguez M, et al. Point-of-care detection of extracellular vesicles: sensitivity optimization and multiple-target detection. *Biosens Bioelectron*. 2017;87:38–45.
33. Vanpouille C, et al. HIV-1 Nef is carried on the surface of extracellular vesicles. *J Extracell Vesicles*. 2024;13(7), e12478.
34. Bystryak S, Acharya C. Detection of HIV-1 p24 antigen in patients with varying degrees of viremia using an ELISA with a photochemical signal amplification system. *Clin Chim Acta*. 2016;456:128–136.
35. Kim Y, et al. Extracellular vesicles from infected cells are released prior to virion release. *Cells*. 2021;10(4).
36. McNamara RP, et al. Nef secretion into extracellular vesicles or exosomes is conserved across human and simian immunodeficiency viruses. *mBio*. 2018;9(1).
37. Roeth JF, Collins KL. Human immunodeficiency virus type 1 Nef: adapting to intracellular trafficking pathways. *Microbiol Mol Biol Rev*. 2006;70(2):548–563.
38. Arenaccio C, et al. Exosomes from human immunodeficiency virus type 1 (HIV-1)-infected cells license quiescent CD4+ T lymphocytes to replicate HIV-1 through a Nef- and ADAM17-dependent mechanism. *J Virol*. 2014;88(19):11529–11539.
39. Raymond AD, et al. HIV Type 1 Nef is released from infected cells in CD45(+) microvesicles and is present in the plasma of HIV-infected individuals. *AIDS Res Hum Retrovir*. 2011;27(2):167–178.
40. DeMarino C, et al. Antiretroviral drugs alter the content of extracellular vesicles from HIV-1-Infected cells. *Sci Rep*. 2018;8(1):7653.
41. Omidfar K, Riahi F, Kashanian S. Lateral flow assay: a summary of recent progress for improving assay performance. *Biosensors (Basel)*. 2023;13(9).